

# Dynamic translocation of ligand-complexed DNA through solid-state nanopores with optical tweezers

Andy Sischka<sup>1,4</sup>, Andre Spiering<sup>1</sup>, Maryam Khaksar<sup>2</sup>,  
Miriam Laxa<sup>3</sup>, Janine König<sup>3</sup>, Karl-Josef Dietz<sup>3</sup> and  
Dario Anselmetti<sup>1</sup>

<sup>1</sup> Experimental Biophysics and Applied Nanoscience, Faculty of Physics, Bielefeld University, D-33615 Bielefeld, Germany

<sup>2</sup> Fachbereich Physik, University of Konstanz, Fach 688, D-78457 Konstanz, Germany

<sup>3</sup> Biochemistry and Plant Physiology, Faculty of Biology, Bielefeld University, D-33615 Bielefeld, Germany

E-mail: [andy.sischka@physik.uni-bielefeld.de](mailto:andy.sischka@physik.uni-bielefeld.de)


Received 21 April 2010, in final form 28 June 2010

Published 29 October 2010

Online at [stacks.iop.org/JPhysCM/22/454121](http://stacks.iop.org/JPhysCM/22/454121)

## Abstract

We investigated the threading and controlled translocation of individual lambda-DNA ( $\lambda$ -DNA) molecules through solid-state nanopores with piconewton force sensitivity, millisecond time resolution and picoampere ionic current sensitivity with a set-up combining quantitative 3D optical tweezers (OT) with electrophysiology. With our virtually interference-free OT set-up the binding of RecA and single peroxiredoxin protein molecules to  $\lambda$ -DNA was quantitatively investigated during dynamic translocation experiments where effective forces and respective ionic currents of the threaded DNA molecule through the nanopore were measured during inward and outward sliding. Membrane voltage-dependent experiments of reversible single protein/DNA translocation scans yield hysteresis-free, asymmetric single-molecule fingerprints in the measured force and conductance signals that can be attributed to the interplay of optical trap and electrostatic nanopore potentials. These experiments allow an exact localization of the bound protein along the DNA strand and open fascinating applications for label-free detection of DNA-binding ligands, where structural and positional binding phenomena can be investigated at a single-molecule level.

 Online supplementary data available from [stacks.iop.org/JPhysCM/22/454121/mmedia](http://stacks.iop.org/JPhysCM/22/454121/mmedia)

(Some figures in this article are in colour only in the electronic version)

## 1. Introduction

Nanopores (NP) have rapidly evolved into a new and promising technique in single-molecule detection, and have been utilized in a variety of set-ups and applications [1–3]. In particular, solid-state NPs with a coulter counter-like detection set-up are a versatile tool to sequentially detect individual DNA molecules [4, 5], distinguish single- and double-stranded nucleic acid molecules [6, 7] and investigate

ligand-complexed DNA strands [8–10]. In a NP coulter counter set-up a large number of stochastic translocation events are monitored and analysed in time-resolved conductance experiments [11, 12]. Although possible statistical effects from different molecular subpopulations or structurally different molecules may affect bioanalytical interpretation, structural properties of translocating molecules can be impressively investigated [11, 12]. In contrast to these sequential and numerable ensemble experiments, the repetitive threading of a distinct individual DNA molecule into a nanopore with nanomanipulation was introduced by Dekker *et al.*, opening a novel and fascinating research area [9, 11, 13].

<sup>4</sup> Address for correspondence: Faculty of Physics, Bielefeld University, Universitaetsstrasse 25, D-33615 Bielefeld, Germany.

The controlled manipulation and threading of individual  $\lambda$ -DNA molecules into a solid-state NP with OT allowed the measurement of (static) effective forces and ionic conductance on naked and protein-coated  $\lambda$ -DNA molecules [11, 13]. However, their published (dynamic) DNA translocation experiment [13], where the DNA molecule was slid through the NP (upon continuously increasing the NP-bead distance), was considerably affected by optical interference effects, which made a proper analysis almost impossible. In order to considerably reduce these interference background effects, we introduced some time ago a novel, virtually interference-free single-beam OT set-up [14].

In this paper, the application of this quantitative OT set-up to investigate the dynamic translocation of individual protein-complexed  $\lambda$ -DNA molecules through solid-state NPs is reported. In membrane voltage-dependent experiments effective forces and ionic currents were simultaneously measured. Asymmetric fingerprints of reversible single protein/DNA translocation scans in the measured signals are presented and discussed in the light of future label-free detection of DNA-binding ligands. Since this paper is part of a special issue about nanopore experiments and also aims to serve as a hands-on experience platform, we would first like to briefly introduce our set-up and the mandatory preparations.

## 2. Optical tweezers set-up

Our quantitative, single-beam 3D OT system [14] is based on an inverted optical microscope allowing axial and lateral manipulation of microbeads in the vicinity of interfaces and uses backscattered light detection for virtual interference-free light detection (figure 1(a)). The P-polarized beam (filled line in figure 1(a)) of an Nd:YAG laser (LCS-DTL-322, Laser 2000, Germany; 1064 nm, 1 W, linear polarized, TEM<sub>00</sub> mode) passes through a polarizing beamsplitter cube (Linios, Germany), is then expanded to a diameter of about 9 mm, passes through a quarter-wave plate (RM-1/4-1046, Newport, CA) changing the linear polarized into right-circular polarized light, and enters the back aperture of the water immersion trapping objective (5.7 mm diameter) with a numerical aperture of 1.2 (UPL-APO60W/IR, Olympus, Japan). The backscattered light (dashed line in figure 1(a)) from the trapped particle (left-circular polarized) is collected by the trapping objective that turns it into a parallel light beam taking the opposite direction through the OT system. The quarter-wave plate changes it into linear S-polarized light, and after passing the beam expander, the light is reflected by the polarizing beamsplitter cube.

For all experiments with solid-state NPs, precise and artefact-free force measurement along the optical axis ( $z$ -direction) is crucial. In our set-up, this is realized by detecting the intensity of the backscattered light, since it can be directly and linearly related to the  $z$ -deflection of the trapped bead with respect to the centre of the optical trap.

Actually, the backscattered light is projected through a 1064 nm long pass filter (RG850, Linios, Germany) onto a photodetector (SD172-11-21-221, Laser Components, Germany). Since this backscattered light from a (low

reflective) membrane is often affected by interference effects [13, 15] we combined our confocal set-up with a central obstruction filter (CO in figure 1(a)) that eliminates the axial light components and therefore significantly reduces interference effects, allowing more precise  $z$ -force measurements [14].

In contrast to our recently described set-up [14], we included a slightly larger CO with a diameter of 2.5 mm and an edge zone of about 0.5 mm where the opacity gradually decreases. Therefore, a maximum trapping force of 35 pN in the  $z$ -direction and an axial trapping stiffness ( $k_{\text{trap}}$ ) of 50 pN  $\mu\text{m}^{-1}$  at 1000 mW laser power output can be achieved when trapping microbeads with a diameter of 3.28  $\mu\text{m}$ . The new CO filter not only forms a ring-like laser beam profile, but also significantly reduces disturbing backscattered light on or close to the optical axis by a factor of up to five in comparison to mere pinhole filtering without CO.

In general, we found that the backscattered set-up is less susceptible to thermal or mechanical drift and misalignments, and yields considerably improved long-term force stability. Moreover, since the upper half-space (above the trapping objective) is not blocked by any force detection devices, integration of a variety of sample chambers is possible without influencing the measurement of small forces in the sub-piconewton range.

## 3. Nanopore sample chamber and electrical contacting

Our custom-made NP sample chamber (figures 1(b) and (d)) [14] encloses a silicon disc (3 mm diameter, thickness of 200  $\mu\text{m}$ ; #4107SN-BA, Structure Probe Inc., PA) that contains a membrane window (20 nm thin Si<sub>3</sub>N<sub>4</sub> membrane with a window size of 60  $\mu\text{m} \times 60 \mu\text{m}$ ). A single NP with a diameter between 15 and 50 nm was milled into the centre of the membrane with a lateral precision of about 2  $\mu\text{m}$  by using a focused-ion-beam machine (Helios NanoLab™, FEI Company, OR). The NP is accessed by a 0.5 mm wide, 26 mm long and 40  $\mu\text{m}$  high channel connecting reservoir 1 with reservoir 2. The silicon disc with the NP is placed centrally on top of this channel while a PDMS ring seals the disc, and a PMMA ring forms reservoir 3.

Electrical contacting was accomplished by immersing platinum wires in a cyanoferrate salt solution (20 mM KCl, 2 mM Tris/HCl, 2 mM K<sub>4</sub>[Fe<sup>II</sup>(CN)<sub>6</sub>], 2 mM K<sub>3</sub>[Fe<sup>III</sup>(CN)<sub>6</sub>], pH 8.0) inside a small glass tube that is confined by agarose gel (1.5% agarose, 98.5% cyanoferrate salt solution) working as a salt bridge. This cyanoferrate salt bridge, in turn, is in contact with another agarose gel salt bridge (1.5% agarose, 98.5% NP buffer) inside a glass tube immersed in reservoirs 1 and 3 to form the electrical contact.

For applying a membrane voltage to the reservoirs and measuring the ionic current with picoampere precision, a patch-clamp amplifier (Axopatch 200B, Molecular Devices, CA) operated in voltage-clamp mode was used, as the headstage of the Axopatch amplifier, and the entire sample chamber were shielded by a Faraday cage.

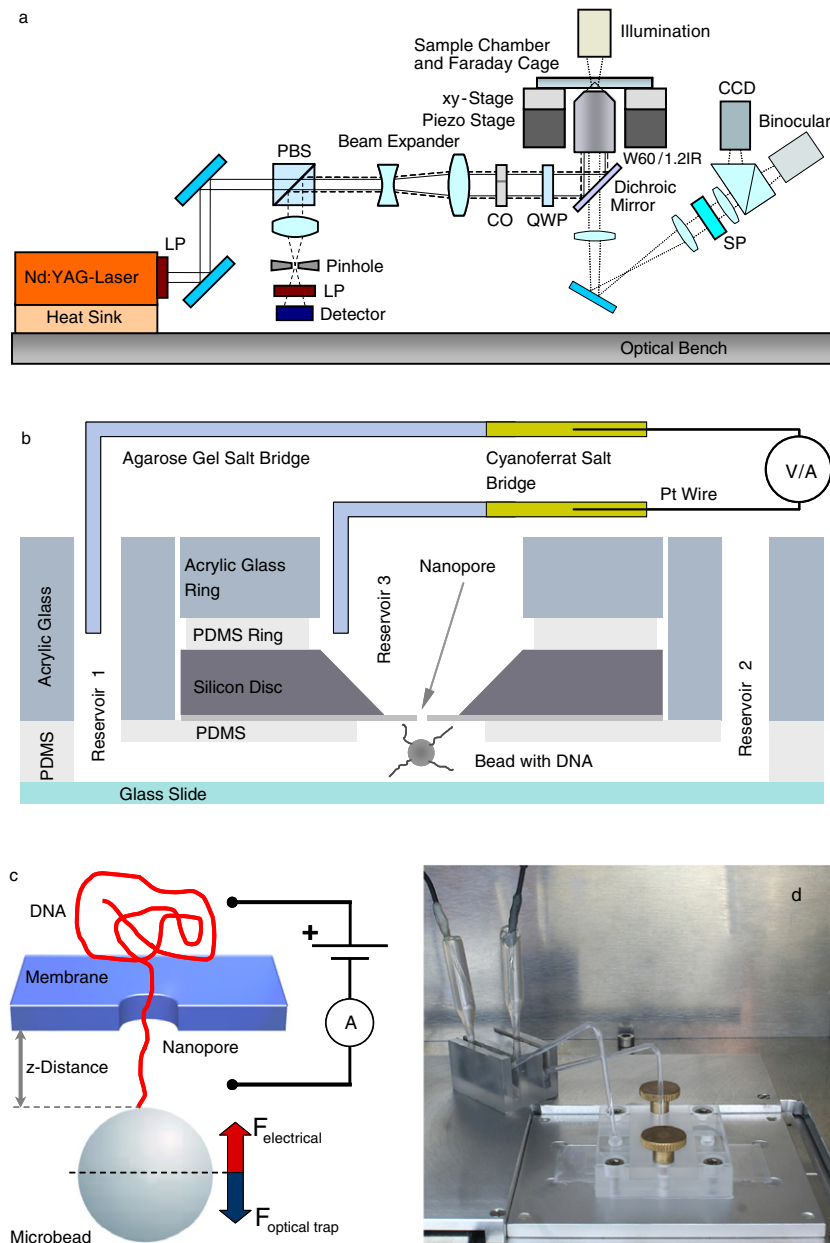


**Figure 1.** (a) 3D quantitative single-beam optical tweezers set-up. The backscatter mode of operation allows easy access to a versatile sample chamber on top of the stage. Abbreviations: LP: 1064 nm long pass filter. PBS: polarizing beamsplitter cube. SP: short pass filter for visual light. QWP: quarter-wave plate. CO: central obstruction filter. Dashed lines indicate backscattered laser light, dotted lines indicate visible light. (b) Set-up of the NP sample chamber. Reservoir 1 and 2 are connected by a small channel, through which the bead–DNA constructs are guided. The bead is trapped underneath the NP. The membrane voltage is applied between reservoirs 1 and 3. The reservoirs are electrically contacted by two agarose gel salt bridges connected to cyanoferrate salt bridges with embedded platinum wires (see section 3 for details). (c) In static mode of operation, an equilibrium between electrostatic and optical force holds the threaded DNA inside the NP. The indicated  $z$ -distance (which can be measured directly with the piezo stage) is defined as the distance between the upper edge of the trapped bead and the nanopore if  $F_{\text{electrical}} = 0$ ; otherwise the  $z$ -distance is slightly reduced by the deflection of the bead according to  $\Delta z = F_{\text{electrical}}/k_{\text{trap}}$ . (d) Photo of the sample chamber with its electrical contacting inside the Faraday cage.

#### 4. Materials and preparative procedures: beads, DNA, RecA and 2-CysPrx

We used monodisperse streptavidin-coated polystyrene beads (3.28  $\mu\text{m}$  diameter; Spherotech, IL; stock concentration of 0.5% w/v) that were diluted by a factor of 1:3000 in NP buffer. The force calibration and all experiments were conducted at

room temperature (22  $^{\circ}\text{C}$ ) in NP buffer (20 mM KCl and 2 mM Tris/HCl at pH 8.0). Forces were calibrated by trapping one microbead suspended in the sample chamber and by moving the piezo stage with a defined velocity in the  $z$ -directions while recording the force signal that was correlated with the hydrodynamic friction according to Stokes' law [16].  $\lambda$ -DNA (48 502 base pairs, 16.4  $\mu\text{m}$  contour length; Promega Corp.,

WI) labelled with multiple biotin molecules on one end is prepared as follows: 66  $\mu\text{l}$  of  $\lambda$ -DNA (New England Biolabs Inc., MA) is denaturated for 15 min at 75 °C and cooled down for 5 min on ice. Ten microlitres of buffer with 50 mM Tris/HCl, 10 mM MgCl<sub>2</sub>, 10 mM DTT, 1 mM ATP and 25  $\mu\text{g}$  BSA is added, as well as 3.4  $\mu\text{l}$  of 5'-GGG CGG CGA CCT-3'-multi-biotin oligonucleotides (Thermo Hybrid Inc., NM), 3.4  $\mu\text{l}$  of 5'-AGG TCG CCG CCC-3' oligonucleotides (MWG Biotech AG, Germany) and 17.2  $\mu\text{l}$  pure water. This solution was incubated for 1 h at 50 °C. Removal of strand nicks was done by adding 3.4  $\mu\text{l}$  T4 ligase stock solution (New England Biolabs Inc., MA), 10  $\mu\text{l}$  ATP (10 mM stock solution) and subsequent incubation for 30 min at 25 °C. The solution was washed using a NICK column (Amersham Pharmacia Biosciences, UK) for purification and stored as a multi-biotin-DNA solution of 5 ng  $\mu\text{l}^{-1}$  in TBE buffer.

For the preparation of DNA-bead constructs, 0.5  $\mu\text{l}$  bead stock solution, 10  $\mu\text{l}$  NP buffer and 4  $\mu\text{l}$  multi-biotin-DNA solution was incubated for 1 h at 6 °C, then washed (adding 1 ml NP buffer and centrifugation for 5 min at 10 000g) and resuspended in 1 ml NP buffer.

Recombination protein A (RecA, New England Biolabs Inc., MA) was complexed with dsDNA according to a protocol adapted from here [12]. 4  $\mu\text{l}$  of multi-biotin-DNA solution, 0.5  $\mu\text{l}$  bead stock solution and 10  $\mu\text{l}$  NP buffer were incubated for 1 h at 6 °C. Consecutively, 20  $\mu\text{l}$  of reaction buffer (1.1 M KCl, 16 mM MgCl<sub>2</sub>, pH 8), 10  $\mu\text{l}$  of 860  $\mu\text{M}$  ATP $\gamma$ S solution (Roche Inc.) and 0.4  $\mu\text{l}$  of 53  $\mu\text{M}$  RecA solution were incubated for 1 h at 37 °C, then washed by centrifugation and resuspended in 1 ml NP buffer.

In contrast to RecA proteins, which are known to form stable nucleoprotein filaments on dsDNA in a cooperative manner [17], 2-cysteine peroxiredoxin (2-CysPrx), an antioxidant enzymatic protein that is supposed to unspecifically bind to DNA, was chosen for our single-molecule experiments. Since a detailed description of peroxiredoxin function [18], preparation and purification procedure [19], as well as DNA-binding analysis of peroxiredoxin somewhat exceeds the scope of this paper, we added preparative and analytical details in the supplementary material section (available at [stacks.iop.org/JPhysCM/22/454121/mmedia](http://stacks.iop.org/JPhysCM/22/454121/mmedia)).

DNA-2-CysPrx-bead constructs were prepared by incubating 4  $\mu\text{l}$  multi-biotin-DNA solution, 0.5  $\mu\text{l}$  bead stock solution (72  $\mu\text{M}$ ), 10  $\mu\text{l}$  PBS buffer (136 mM NaCl, 2.7 mM KCl, 8.1 mM Na<sub>2</sub>HPO<sub>4</sub> and 1.5 mM KH<sub>2</sub>PO<sub>4</sub> at pH 7.4) and 5  $\mu\text{l}$  2-CysPrx-A stock solution (70  $\mu\text{M}$ ) for 2 h at 22 °C. Subsequently, this solution was washed by centrifugation and resuspended in 1 ml NP buffer.

## 5. Proof of principle: dynamic translocation of dsDNA and RecA-complexed dsDNA through a nanopore

When a positive voltage (typically +50 mV) is applied across the Si<sub>3</sub>N<sub>4</sub> membrane, a DNA molecule, which is attached to a microbead in the vicinity of the NP, is immediately threaded into the NP by electrostatic forces (figure 1(c)). The threading

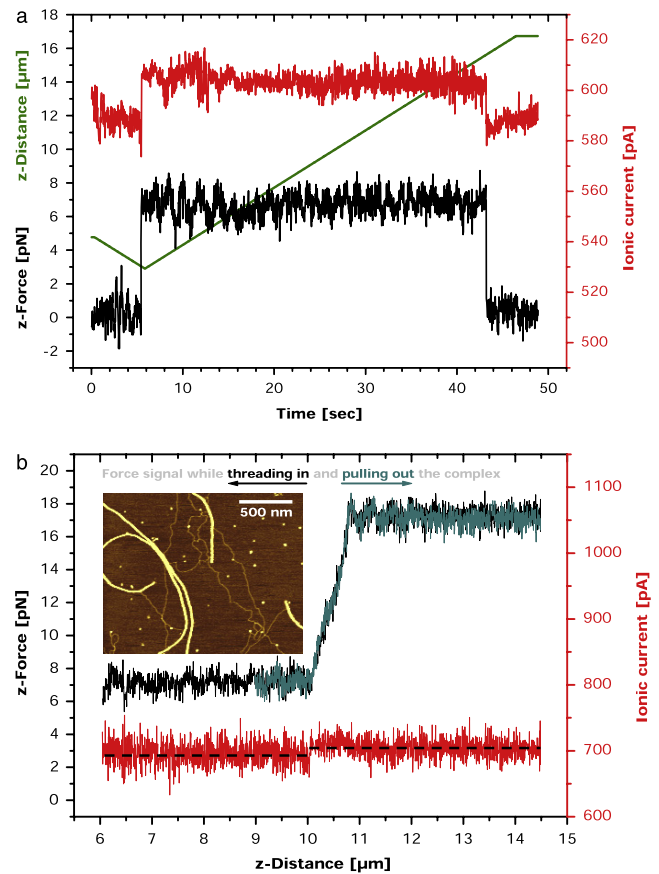


**Figure 2.** (a) The threading of a single  $\lambda$ -DNA molecule into a NP with a diameter of 30 nm can be detected by a simultaneous step in the force and the ionic current signals. Upon linearly increasing the  $z$ -distance (green line) at a constant velocity of 0.35  $\mu\text{m s}^{-1}$  in the dynamic translocation mode of operation, effective forces (black line) and NP conductance (red line) remain at a constant level until the DNA is completely threaded out of the pore at a distance of 15.6  $\mu\text{m}$ . The applied voltage was +50 mV. (b) Dynamic translocation of a single DNA-RecA filament inward (black line) and outward (blue line) of the NP (NP diameter: 40 nm). For an applied voltage of +50 mV, a steep increase in the force signal from 7 to 17 pN and a simultaneous step of the ionic current signal by only 10 pA can be observed, which is attributed to the entering of the RecA-coated DNA filament that is threaded through the NP. Inset: AFM image of RecA-dsDNA filaments that are partially coated, immobilized on mica. RecA-coated DNA filaments appear as thicker filaments, whereas thinner strands indicate naked dsDNA.

can be monitored as an abrupt step in the  $z$ -force signal as the molecule is deflecting the bead in the  $+z$ -direction with respect to the optical trap (figure 2(a)).

Typically, the threaded DNA molecule exerts an effective force of about 7 pN that deflects the trapped bead in the  $+z$ -direction. This effective force can quantitatively be understood by an interplay of electrostatic forces (the DNA backbone is negatively charged by two electrons per base pair) and electroosmotic contributions by counterion screening of DNA and NP surfaces that reduce the electrostatic forces by  $\sim 85\%$  [20, 21]. We determined this effective force for an individual dsDNA molecule to be  $0.14 \pm 0.02$  pN  $\text{mV}^{-1}$  and rather independent from the probed NP (diameters: 20–50 nm) and buffer conditions (ionic strength: 20–150 mM

KCl), consistent with recent experiments [14, 21]. It is worth noting that the threading force step is accompanied by a step in the corresponding NP ionic current signal (see also figure 2(a)). We estimated the increase of the current to be of 0.2–0.3 pA mV<sup>-1</sup> and 0.3–0.5 pA mV<sup>-1</sup> for NP diameters of 30–50 nm and 20–30 nm, respectively. The change in NP conductance can be explained by an increased charge carrier density in the NP due to additional cations screening the threaded, negatively charged dsDNA backbone. We found this generally valid for all KCl concentrations well below 400 mM [22], where the attraction of counterions outbalances the behaviour of a DNA molecule to act as an obstacle for the ionic current through the NP.

In dynamic translocation experiments, the bead with the threaded DNA molecule is now retracted from the NP at a constant velocity of 0.35  $\mu\text{m s}^{-1}$  (see figure 2(a): green line), while  $z$ -distance, force and ionic current are monitored. Apparently, the measured effective force and the NP conductance basically remain at a constant level, since a homogeneous fraction of the DNA helix always passes through the pore. Here, the accuracy of the dynamic  $z$ -force measurements is  $\pm 1$  pN, which is the result of the stochastic background noise of molecular Brownian motion and of a weak remaining interference effect between the backscattered light from the bead and from the low reflective membrane [14]. It is noteworthy that the raw data force signals can be post-experiment-corrected from this slight interference effect by fitting and subtracting an overall and uniform harmonic function from the measured data.

At a distance of 15.6  $\mu\text{m}$ , the DNA strand is completely threaded out of the NP, indicated by a sudden step in the force and ionic current signals to its original baseline value. In order to estimate the DNA contour length according to a straightforward worm-like-chain (WLC) polymer elasticity calculation [23] first the measured end-to-end distance of 15.6  $\mu\text{m}$  has to be corrected by the  $z$ -deflection of the bead within the OT potential due to the effective force. Assuming a persistence length of  $l_p \cong 50$  nm in 20 mM KCl solution [24] and an external force of 7 pN, a nominal contour length of  $L_C = 16.3 \mu\text{m}$  can be deduced which nicely complies with the literature value for  $\lambda$ -DNA ( $L_C(\lambda\text{-DNA}) = 16.4 \mu\text{m}$ ).

Since diameter and surface charge of a threaded polymer influence the measured effective forces and NP conductance, we additionally investigated the threading of a single DNA–RecA complex where double-stranded  $\lambda$ -DNA is partially coated with RecA and forms nucleoprotein filaments (see the inset of figure 2(b)) [11, 17]. Such a successful threading experiment is shown in figure 2(b) (NP diameter 40 nm, membrane voltage +50 mV), where effective forces and ionic currents are plotted in a dynamic translocation scan (for in- and outward threading). Whereas on the left part of the force curve the average force level remains at about 7 pN which indicates that a naked  $\lambda$ -DNA molecule is inside the NP, a steep force increase at  $z = 10.1 \mu\text{m}$  to about 17 pN can be observed. This transition to a larger effective force can be repetitively reproduced many times for various velocities (0.1–2  $\mu\text{m s}^{-1}$ ) and reflects the penetration of the NP by the RecA-coated DNA filament that is characterized by a larger negative surface charge [25, 11].

Interestingly, only a minor change in the ionic current could be detected, as can be seen in figure 2(b). This is attributed to the fact that the 7–12 nm thick RecA filament [26, 27] acts on the one hand as an obstacle for the ionic current, reducing the effective cross-sectional area of the pore and therefore leading to a reduced conductance and, on the other hand leads to an increased counterion charge carrier density in the NP and therefore to an increased ionic current. Obviously, both opposing effects are apparent and compensate each other almost fully for pore diameters of 25–40 nm.

## 6. Dynamic translocation of a single DNA–2-CysPrx complex

In contrast to the cooperative formation of long nucleoprotein filaments by RecA, we chose 2-CysPrx molecules in order to investigate the dynamic threading of an isolated single molecule bound to DNA through a NP. In figure 3(a) force and ionic current are shown where a single 2-CysPrx protein is attached to a  $\lambda$ -DNA strand that was dynamically scanned inwards and outwards of the NP with a velocity of 0.1  $\mu\text{m s}^{-1}$  at a membrane voltage of +50 mV. Characteristic dips in the effective force and current signals were found in numerous experiments with various  $\lambda$ -DNA molecules—differing only in the  $z$ -distance location on the DNA molecule—which we attributed to individual positively charged 2-CysPrx unspecifically bound to the  $\lambda$ -DNA strand.

In figure 3(b) the characteristic force fingerprint of a single 2-CysPrx/DNA-complex threaded through a 35 nm NP is shown for three different membrane voltages which were measured in consecutive scans. Clearly, the effective DNA force ( $F_{\text{dsDNA}}$ ) as well as the depth of the characteristic signal dip ( $F_{\text{ligand}}$ ) increase, yielding an improved signal-to-noise ratio at larger voltages. A quantitative analysis of the membrane voltage dependence of  $F_{\text{dsDNA}}$  and  $F_{\text{ligand}}$  is shown in figure 3(c), where a linear dependence of  $F_{\text{dsDNA}}$  and  $F_{\text{ligand}}$  with an overall force reduction to  $F_{\text{ligand}}/F_{\text{dsDNA}} = 62 \pm 3\%$  for all voltages between 30 and 150 mV—independent of the translocation velocity or direction—could be found.

Although the 2-CysPrx is firmly bound to DNA, an apparent shift of the exact binding  $z$ -location can be detected. This shift to larger  $z$ -distance values with larger membrane voltages reflects the fact that the threaded DNA is subjected to larger forces and reacts as an elastic polymer by partial elongation. In a quantitative analysis, the measured voltage-dependent binding locations of the 2-CysPrx at 6.88  $\mu\text{m}$ , 7.01  $\mu\text{m}$  and 7.19  $\mu\text{m}$  for +30, +50 and +80 mV, respectively, have first to be corrected by the displacement of the bead within the optical trap due to the different effective forces (4.8, 7.3 and 12.4 pN). Thus, the corrected distances of 6.78  $\mu\text{m}$ , 6.86  $\mu\text{m}$  and 6.94  $\mu\text{m}$ , respectively, can now be analysed within the framework of a WLC elastic polymer model, yielding a ‘true’ distance of 7.24  $\mu\text{m}$  (which is equivalent to the contour length in the WLC model) between the end of the DNA molecule attached to the bead and the location of the 2-CysPrx molecule. This analytical correction is very important in future experiments with an OT/NP set-up, where exact structural and positional binding phenomena will be analysed at the single-molecule level.

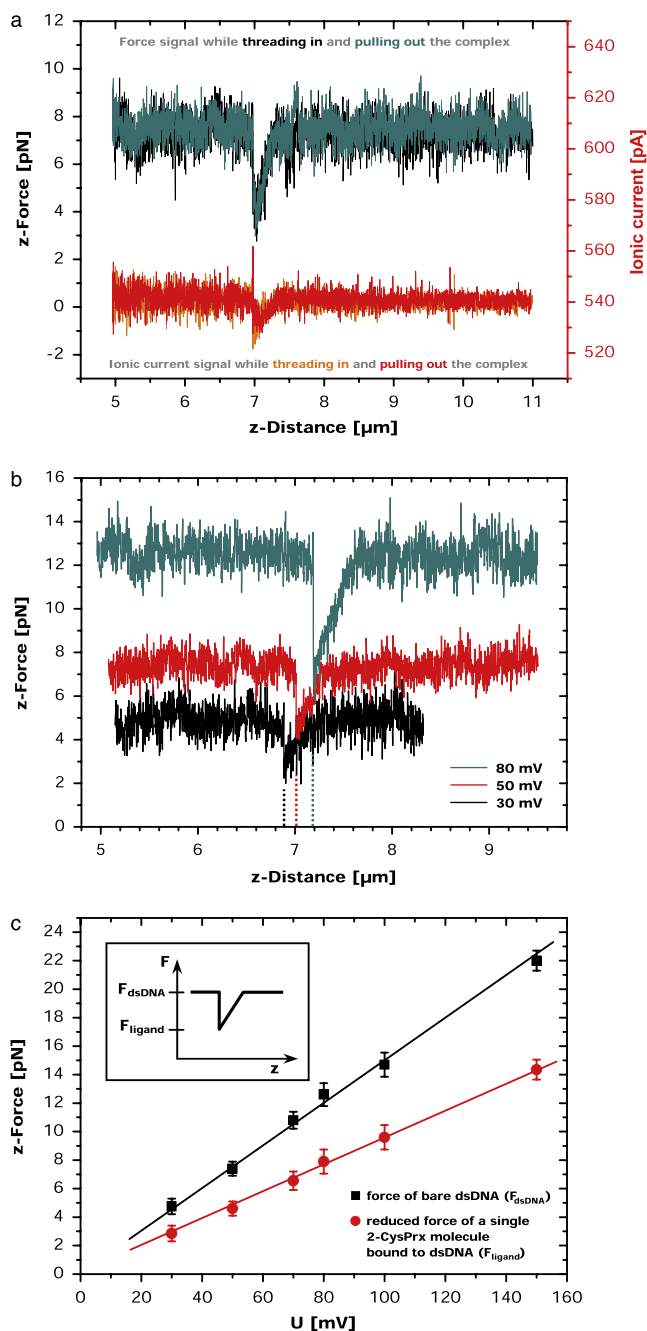


**Figure 3.** (a) Simultaneous force and current signals, when a single 2-CysPrx molecule bound to  $\lambda$ -DNA is dynamically threaded through the NP. Individual in- and outward threading events (membrane voltage: +50 mV, sliding velocity:  $0.1 \mu\text{m s}^{-1}$ ) reproducibly exhibit a distinct force dip at a  $z$ -distance of  $7.0 \mu\text{m}$ . (b) Force signals of a NP-threaded 2-CysPrx- $\lambda$ -DNA complex taken at different membrane voltages. An apparent shift of the exact binding  $z$ -location with larger voltages can be detected (dotted lines) that reflects the elastic response of a polymer under an external force. (c) Voltage dependence of the effective force acting on naked dsDNA ( $F_{\text{dsDNA}}$ , black squares), as well as the reduced forces induced by a single 2-CysPrx molecule attached to DNA ( $F_{\text{ligand}}$ , red dots).

Another interesting aspect concerns the asymmetric  $z$ -distance profiles measured in the effective force and conductance signals (figures 3(a) and (b)). This fingerprint

was always found to be independent of the sliding direction or velocity. In particular, the single-molecule force signal dips are characterized by a sharp edge at lower  $z$ -distances and a rather gradual progression extending up to 300 nm to larger  $z$ -distance values largely exceeding the size of the bound protein molecule (at +50 mV). This indicates that, just before the positively charged 2-CysPrx protein gets threaded through the pore, the equilibrium between the electrostatic and optical trapping forces is becoming unstable due to a larger force gradient of the electrostatic NP potential that exceeds the combined force constant of trap stiffness and dsDNA elasticity. A very similar phenomenon is also well known in atomic force microscopy as the ‘jump to contact’ of the force sensor in the vicinity of a surface in the attractive force regime [28].

## 7. Conclusions

The controlled threading and dynamic translocation of DNA and ligand-complexed DNA (RecA and 2-CysPrx) through solid-state nanopores was investigated by a combination of quantitative 3D OT and electrophysiology. In contrast to previous set-ups, our single-beam OT system combines confocal pinhole-based filtering and spatial filtering by using a central obstruction filter, which allows virtually interference-free (artefact-free) and dynamic force experiments in the vicinity of thin solid-state membranes and nanopores. The set-up was tested with naked double-stranded  $\lambda$ -DNA and nucleoprotein RecA/DNA filaments, as well as single-molecule 2-CysPrx-complexed  $\lambda$ -DNA in dynamic translocation experiments, where the distance between optical trap and membrane interface could be controlled and adjusted with nanometre precision. Membrane voltage-dependent experiments of reversible single protein/DNA translocation scans yielded hysteresis-free, asymmetric single-molecule fingerprints in the measured effective force and conductance signals that could be attributed to the interplay of optical trap and electrostatic nanopore potentials. We could show that, with these nanopore force spectroscopy (NPFS) experiments, an exact and reproducible localization of the bound protein along the DNA strand is possible, which enables fascinating applications for label-free detection of DNA-binding ligands, where structural and positional binding phenomena can be quantitatively investigated at a single-molecule level.

## Acknowledgments

We thank Cees Dekker, Harald Fuchs, Thomas Gisler, Wiebke Hachmann, Martin Hegner, Ulrich F Keyser, Tanja Plötz, Karsten Rott, Ina Seuffert, Urs Stauffer and Katja Tönsing for helpful discussions and technical advice. Financial support from the Collaborative Research Centre SFB 613 from the Deutsche Forschungsgemeinschaft (DFG) is gratefully acknowledged.

## References

- [1] Howorka S, Cheley S and Bayley H 2001 *Nat. Biotechnol.* **19** 636
- [2] Nakane J J, Akeson M and Marziali A 2003 *J. Phys.: Condens. Matter* **15** R1365

- [3] Howorka S and Siwy Z 2009 *Chem. Soc. Rev.* **38** 2360
- [4] Keyser U F, Koeleman B N, van Dorp S, Krapf D, Smeets R M M, Lemay S G, Dekker N H and Dekker C 2006 *Nat. Phys.* **2** 473
- [5] Wanunu M, Sutin J, McNally B, Chow A and Meller A 2008 *Biophys. J.* **95** 4716
- [6] Skinner G M, van den Hout M, Broekmans O, Dekker C and Dekker N H 2009 *Nano Lett.* **9** 2953
- [7] van den Hout M, Vilfan I D, Hage S and Dekker N H 2010 *Nano Lett.* **10** 701
- [8] Petrossian L, Wilk S J, Joshi P, Goodnick S M and Thornton T J 2008 *J. Phys.: Conf. Ser.* **109** 012028
- [9] Smeets R M, Kowalczyk S W, Hall A R, Dekker N H and Dekker C 2009 *Nano Lett.* **9** 3089
- [10] Wanunu M, Sutin J and Meller A 2009 *Nano Lett.* **10** 3498
- [11] Hall A R, van Dorp S, Lemay S G and Dekker C 2009 *Nano Lett.* **9** 4441
- [12] Kowalczyk S W, Hall A R and Dekker C 2010 *Nano Lett.* **10** 324
- [13] Keyser U F, van der Does J, Dekker C and Dekker N H 2006 *Rev. Sci. Instrum.* **77** 105105
- [14] Sischka A, Kleimann C, Hachmann W, Schäfer M M, Seuffert I, Tönsing K and Anselmetti D 2008 *Rev. Sci. Instrum.* **79** 063702
- [15] Jonas A, Zemanek P and Florin E L 2001 *Opt. Lett.* **26** 1466
- [16] Ghislain L P, Switz N A and Webb W W 1994 *Rev. Sci. Instrum.* **65** 2762
- [17] Roca A I and Cox M M 1997 *Prog. Nucl. Acid Res. Mol. Biol.* **56** 129
- [18] Muthuramalingam M, Seidel T, Laxa M, de Miranda S M N, Gärtner F, Ströher E, Kandlbinder A and Dietz K J 2009 *Mol. Plant* **2** 1273
- [19] König J, Lotte K, Plessow R, Brockhinke A, Baier M and Dietz K J 2003 *J. Biol. Chem.* **278** 24409
- [20] Luan B and Aksimentiev A 2008 *Phys. Rev. E* **78** 021912
- [21] van Dorp S, Keyser U F, Dekker N H, Dekker C and Lemay S G 2009 *Nat. Phys.* **5** 347
- [22] Smeets R M, Keyser U F, Krapf D, Wu M Y, Dekker N H and Dekker C 2006 *Nano Lett.* **6** 89
- [23] Marko J F and Siggia E D 1995 *Macromolecules* **28** 8759
- [24] Wenner J R, Williams M C, Rouzina I and Bloomfield V A 2002 *Biophys. J.* **82** 3160
- [25] Simonson T, Kubista M, Sjoback R, Ryberg H and Takahashi M 1994 *J. Mol. Recog.* **7** 199
- [26] Dunn K, Chrysogelos S and Griffith J 1982 *Cell* **28** 757
- [27] Chen Z, Yang H and Pavletich N P 2008 *Nature* **453** 489
- [28] Morita S, Wiesendanger R and Meyer E 2002 *Noncontact Atomic Force Microscopy* (Berlin: Springer)